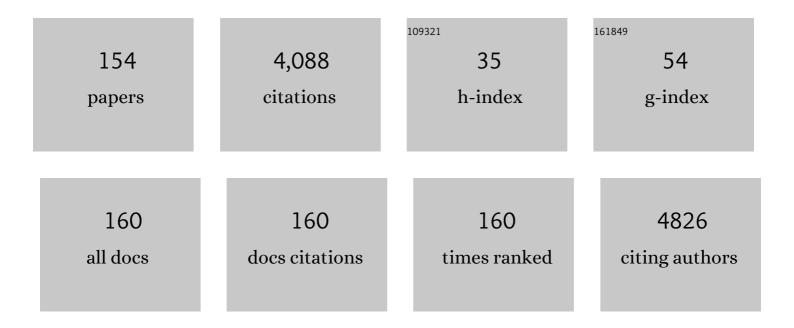
## Julio Caballero

List of Publications by Year in descending order

Source: https://exaly.com/author-pdf/7267820/publications.pdf Version: 2024-02-01



#	Article	IF	CITATIONS
1	Is It Reliable to Take the Molecular Docking Top Scoring Position as the Best Solution without Considering Available Structural Data?. Molecules, 2018, 23, 1038.	3.8	267
2	ls It Reliable to Use Common Molecular Docking Methods for Comparing the Binding Affinities of Enantiomer Pairs for Their Protein Target?. International Journal of Molecular Sciences, 2016, 17, 525.	4.1	114
3	Immobilization of Adamantane-Modified Cytochromecat Electrode Surfaces through Supramolecular Interactions. Langmuir, 2002, 18, 5051-5054.	3.5	88
4	Quantitative structure–activity relationship to predict differential inhibition of aldose reductase by flavonoid compounds. Bioorganic and Medicinal Chemistry, 2005, 13, 3269-3277.	3.0	87
5	LigRMSD: a web server for automatic structure matching and RMSD calculations among identical and similar compounds in protein-ligand docking. Bioinformatics, 2020, 36, 2912-2914.	4.1	84
6	Genetic algorithm optimization in drug design QSAR: Bayesian-regularized genetic neural networks (BRGNN) and genetic algorithm-optimized support vectors machines (GA-SVM). Molecular Diversity, 2011, 15, 269-289.	3.9	81
7	QSAR for non-nucleoside inhibitors of HIV-1 reverse transcriptase. Bioorganic and Medicinal Chemistry, 2006, 14, 5876-5889.	3.0	80
8	Minimizing the Risk of Reporting False Aromaticity and Antiaromaticity in Inorganic Heterocycles Following Magnetic Criteria. Inorganic Chemistry, 2014, 53, 3579-3585.	4.0	80
9	Chlorogenic Acid Inhibits Human Platelet Activation and Thrombus Formation. PLoS ONE, 2014, 9, e90699.	2.5	78
10	Linear and nonlinear modeling of antifungal activity of some heterocyclic ring derivatives using multiple linear regression and Bayesian-regularized neural networks. Journal of Molecular Modeling, 2006, 12, 168-181.	1.8	73
11	Artificial Neural Networks from MATLAB® in Medicinal Chemistry. Bayesian-Regularized Genetic Neural Networks (BRGNN): Application to the Prediction of the Antagonistic Activity Against Human Platelet Thrombin Receptor (PAR-1). Current Topics in Medicinal Chemistry, 2008, 8, 1580-1605.	2.1	72
12	Study of the Differential Activity of Thrombin Inhibitors Using Docking, QSAR, Molecular Dynamics, and MM-GBSA. PLoS ONE, 2015, 10, e0142774.	2.5	70
13	Linear and nonlinear QSAR study of N-hydroxy-2-[(phenylsulfonyl)amino]acetamide derivatives as matrix metalloproteinase inhibitors. Bioorganic and Medicinal Chemistry, 2006, 14, 4137-4150.	3.0	63
14	Inhibition of Platelet Activation and Thrombus Formation by Adenosine and Inosine: Studies on Their Relative Contribution and Molecular Modeling. PLoS ONE, 2014, 9, e112741.	2.5	63
15	Rosmarinic acid prevents fibrillization and diminishes vibrational modes associated to β sheet in tau protein linked to Alzheimer's disease. Journal of Enzyme Inhibition and Medicinal Chemistry, 2017, 32, 945-953.	5.2	63
16	Modeling of farnesyltransferase inhibition by some thiol and non-thiol peptidomimetic inhibitors using genetic neural networks and RDF approaches. Bioorganic and Medicinal Chemistry, 2006, 14, 200-213.	3.0	62
17	3D-QSAR (CoMFA and CoMSIA) and pharmacophore (GALAHAD) studies on the differential inhibition of aldose reductase by flavonoid compounds. Journal of Molecular Graphics and Modelling, 2010, 29, 363-371.	2.4	61
18	Modeling of activity of cyclic urea HIV-1 protease inhibitors using regularized-artificial neural networks. Bioorganic and Medicinal Chemistry, 2006, 14, 280-294.	3.0	60

#	Article	IF	CITATIONS
19	Rationalizing the stability and interactions of 2,4-diamino-5-(4-chlorophenyl)-6-ethylpyrimidin-1-ium 2-hydroxy-3,5-dinitrobenzoate salt. Journal of Molecular Structure, 2019, 1193, 185-194.	3.6	60
20	Study of Interaction Energies between the PAMAM Dendrimer and Nonsteroidal Anti-Inflammatory Drug Using a Distributed Computational Strategy and Experimental Analysis by ESI-MS/MS. Journal of Physical Chemistry B, 2012, 116, 2031-2039.	2.6	59
21	Performance of the MM/GBSA scoring using a binding site hydrogen bond network-based frame selection: the protein kinase case. Physical Chemistry Chemical Physics, 2014, 16, 14047-14058.	2.8	58
22	Amino Acid Sequence Autocorrelation Vectors and Ensembles of Bayesian-Regularized Genetic Neural Networks for Prediction of Conformational Stability of Human Lysozyme Mutants. Journal of Chemical Information and Modeling, 2006, 46, 1255-1268.	5.4	57
23	Insights into the Structural Basis of N2 and O6 Substituted Guanine Derivatives as Cyclin-Dependent Kinase 2 (CDK2) Inhibitors: Prediction of the Binding Modes and Potency of the inhibitors by Docking and ONIOM Calculations. Journal of Chemical Information and Modeling, 2009, 49, 886-899.	5.4	57
24	Modeling of Cyclin-Dependent Kinase Inhibition by 1H-Pyrazolo[3,4-d]Pyrimidine Derivatives Using Artificial Neural Network Ensembles. Journal of Chemical Information and Modeling, 2005, 45, 1884-1895.	5.4	54
25	Proteometric study of ghrelin receptor function variations upon mutations using amino acid sequence autocorrelation vectors and genetic algorithm-based least square support vector machines. Journal of Molecular Graphics and Modelling, 2007, 26, 166-178.	2.4	53
26	Protective mechanisms of adenosine 5′-monophosphate in platelet activation and thrombus formation. Thrombosis and Haemostasis, 2014, 111, 491-507.	3.4	52
27	Secondary Metabolites in Ramalina terebrata Detected by UHPLC/ESI/MS/MS and Identification of Parietin as Tau Protein Inhibitor. International Journal of Molecular Sciences, 2016, 17, 1303.	4.1	50
28	Amino acid sequence autocorrelation vectors and bayesian-regularized genetic neural networks for modeling protein conformational stability: Gene V protein mutants. Proteins: Structure, Function and Bioinformatics, 2007, 67, 834-852.	2.6	46
29	Identification of a potent and selective σ1 receptor agonist potentiating NGF-induced neurite outgrowth in PC12 cells. Bioorganic and Medicinal Chemistry, 2011, 19, 6210-6224.	3.0	45
30	Study of differences in the VEGFR2 inhibitory activities between semaxanib and SU5205 using 3D-QSAR, docking, and molecular dynamics simulations. Journal of Molecular Graphics and Modelling, 2012, 32, 39-48.	2.4	44
31	QSAR analysis for heterocyclic antifungals. Bioorganic and Medicinal Chemistry, 2007, 15, 2680-2689.	3.0	42
32	Supramolecular assembly of β-cyclodextrin-modified gold nanoparticles and Cu, Zn-superoxide dismutase on catalase. Journal of Molecular Catalysis B: Enzymatic, 2005, 35, 79-85.	1.8	41
33	QSAR modeling of matrix metalloproteinase inhibition by N-hydroxy-α-phenylsulfonylacetamide derivatives. Bioorganic and Medicinal Chemistry, 2007, 15, 6298-6310.	3.0	40
34	A Novel Class of Selective Acetylcholinesterase Inhibitors: Synthesis and Evaluation of (E)-2-(Benzo[d]thiazol-2-yl)-3-heteroarylacrylonitriles. Molecules, 2012, 17, 12072-12085.	3.8	40
35	Quantitative Structure–Activity Relationship of Rubiscolin Analogues as δOpioid Peptides Using Comparative Molecular Field Analysis (CoMFA) and Comparative Molecular Similarity Indices Analysis (CoMSIA). Journal of Agricultural and Food Chemistry, 2007, 55, 8101-8104.	5.2	36
36	Bayesian-regularized genetic neural networks applied to the modeling of non-peptide antagonists for the human luteinizing hormone-releasing hormone receptor. Journal of Molecular Graphics and Modelling, 2006, 25, 410-422.	2.4	35

#	Article	IF	CITATIONS
37	Considerations for Docking of Selective Angiotensin-Converting Enzyme Inhibitors. Molecules, 2020, 25, 295.	3.8	35
38	1,3-Dipolar cycloaddition of nitrile imines with α,β-unsaturated lactones, thiolactones and lactams: synthesis of ring-fused pyrazoles. Tetrahedron, 2012, 68, 3319-3328.	1.9	34
39	Design, synthesis and cellular dynamics studies in membranes of a new coumarin-based "turn-off― fluorescent probe selective for Fe2+. European Journal of Medicinal Chemistry, 2013, 67, 60-63.	5.5	34
40	Modeling of the Inhibition Constant (Ki) of Some Cruzain Ketone-Based Inhibitors Using 2D Spatial Autocorrelation Vectors and Data-Diverse Ensembles of Bayesian-Regularized Genetic Neural Networks. QSAR and Combinatorial Science, 2007, 26, 27-40.	1.4	33
41	Computational Study on the Interaction of N1 Substituted Pyrazole Derivatives with B-Raf Kinase: An Unusual Water Wire Hydrogen-Bond Network and Novel Interactions at the Entrance of the Active Site. Journal of Chemical Information and Modeling, 2010, 50, 1101-1112.	5.4	33
42	Structural requirements of pyrido[2,3-d]pyrimidin-7-one as CDK4/D inhibitors: 2D autocorrelation, CoMFA and CoMSIA analyses. Bioorganic and Medicinal Chemistry, 2008, 16, 6103-6115.	3.0	32
43	Quality Threshold Clustering of Molecular Dynamics: A Word of Caution. Journal of Chemical Information and Modeling, 2020, 60, 467-472.	5.4	31
44	Docking and Quantitative Structure–Activity Relationship Studies for the Bisphenylbenzimidazole Family of Nonâ€Nucleoside Inhibitors of HIVâ€I Reverse Transcriptase. Chemical Biology and Drug Design, 2008, 72, 360-369.	3.2	30
45	Study of the Interaction between Progesterone and β-Cyclodextrin by Electrochemical Techniques and Steered Molecular Dynamics. Journal of Physical Chemistry B, 2008, 112, 10194-10201.	2.6	30
46	Direct and Auger Electron-Induced, Single- and Double-Strand Breaks on Plasmid DNA Caused by 99mTc-Labeled Pyrene Derivatives and the Effect of Bonding Distance. PLoS ONE, 2016, 11, e0161973.	2.5	30
47	2D Autocorrelation modeling of the activity of trihalobenzocycloheptapyridine analogues as farnesyl protein transferase inhibitors. Molecular Simulation, 2005, 31, 575-584.	2.0	29
48	2D Autocorrelation modeling of the negative inotropic activity of calcium entry blockers using Bayesian-regularized genetic neural networks. Bioorganic and Medicinal Chemistry, 2006, 14, 3330-3340.	3.0	29
49	2D Autocorrelation, CoMFA, and CoMSIA modeling of protein tyrosine kinases' inhibition by substituted pyrido[2,3-d]pyrimidine derivatives. Bioorganic and Medicinal Chemistry, 2008, 16, 810-821.	3.0	29
50	The latest automated docking technologies for novel drug discovery. Expert Opinion on Drug Discovery, 2021, 16, 625-645.	5.0	29
51	2D Autocorrelation Modelling of the Inhibitory Activity of Cytokinin-Derived Cyclin-Dependent Kinase Inhibitors. Bulletin of Mathematical Biology, 2006, 68, 735-751.	1.9	28
52	Insights into the Interactions between Maleimide Derivates and GSK3Î <sup>2</sup> Combining Molecular Docking and QSAR. PLoS ONE, 2014, 9, e102212.	2.5	28
53	Docking and quantitative structure–activity relationship studies for 3-fluoro-4-(pyrrolo[2,1-f][1,2,4]triazin-4-yloxy)aniline, 3-fluoro-4-(1H-pyrrolo[2,3-b]pyridin-4-yloxy)aniline, and 4-(4-amino-2-fluorophenoxy)-2-pyridinylamine derivatives as c-Met kinase inhibitors. Journal of Computer-Aided Molecular Design, 2011, 25, 349-369.	2.9	27
54	Synthesis, in silico, inÂvitro, and inÂvivo investigation of 5-[11C]methoxy-substituted sunitinib, a tyrosine kinase inhibitor of VEGFR-2. European Journal of Medicinal Chemistry, 2012, 58, 272-280.	5.5	27

#	Article	IF	CITATIONS
55	Association of nicotinic acid with a poly(amidoamine) dendrimer studied by molecular dynamics simulations. Journal of Molecular Graphics and Modelling, 2013, 39, 71-78.	2.4	27
56	Flavonoids as CDK1 Inhibitors: Insights in Their Binding Orientations and Structure-Activity Relationship. PLoS ONE, 2016, 11, e0161111.	2.5	27
57	The receptor-like pseudokinase MRH1 interacts with the voltage-gated potassium channel AKT2. Scientific Reports, 2017, 7, 44611.	3.3	25
58	Modeling of acetylcholinesterase inhibition by tacrine analogues using Bayesian-regularized Genetic Neural Networks and ensemble averaging. Journal of Enzyme Inhibition and Medicinal Chemistry, 2006, 21, 647-661.	5.2	23
59	Docking and quantitative structure–activity relationship of oxadiazole derivates as inhibitors of GSK3 \$\$upbeta \$\$ β. Molecular Diversity, 2014, 18, 149-159.	3.9	23
60	Improved Anti-Inflammatory and Pharmacokinetic Properties for Superoxide Dismutase by Chemical Glycosidation with Carboxymethylchitin. Macromolecular Bioscience, 2005, 5, 118-123.	4.1	22
61	Ensembles of Bayesian-regularized Genetic Neural Networks for Modeling of Acetylcholinesterase Inhibition by Huprines. Chemical Biology and Drug Design, 2006, 68, 201-212.	3.2	22
62	Computational Study of the Interactions between Guanine Derivatives and Cyclin-Dependent Kinase 2 (CDK2) by CoMFA and QM/MM. Journal of Chemical Information and Modeling, 2010, 50, 110-122.	5.4	22
63	Insights into the structure of urea-like compounds as inhibitors of the juvenile hormone epoxide hydrolase (IHEH) of the tobacco hornworm Manduca sexta: Analysis of the binding modes and structure–activity relationships of the inhibitors by docking and CoMFA calculations. Chemosphere, 2011. 82. 1604-1613.	8.2	22
64	Computational study of the binding orientation and affinity of PPARÎ <sup>3</sup> agonists: inclusion of ligand-induced fit by cross-docking. RSC Advances, 2016, 6, 64756-64768.	3.6	22
65	Computational Studies of Snake Venom Toxins. Toxins, 2018, 10, 8.	3.4	22
66	Molecular dynamics simulations and CD spectroscopy reveal hydration-induced unfolding of the intrinsically disordered LEA proteins COR15A and COR15B from Arabidopsis thaliana. Physical Chemistry Chemical Physics, 2016, 18, 25806-25816.	2.8	21
67	Folding and Lipid Composition Determine Membrane Interaction of the Disordered Protein COR15A. Biophysical Journal, 2018, 115, 968-980.	0.5	21
68	Omega hydroxylated JA-lle is an endogenous bioactive jasmonate that signals through the canonical jasmonate signaling pathway. Biochimica Et Biophysica Acta - Molecular and Cell Biology of Lipids, 2019, 1864, 158520.	2.4	21
69	Classification of conformational stability of protein mutants from 3D pseudoâ€folding graph representation of protein sequences using support vector machines. Proteins: Structure, Function and Bioinformatics, 2008, 70, 167-175.	2.6	20
70	Molecular Dynamics of Protein Kinase-Inhibitor Complexes: A Valid Structural Information. Current Pharmaceutical Design, 2012, 18, 2946-2963.	1.9	20
71	The pH sensor of the plant K+-uptake channel KAT1 is built from a sensory cloud rather than from single key amino acids. Biochemical Journal, 2012, 442, 57-63.	3.7	20
72	Structural and Affinity Determinants in the Interaction between Alcohol Acyltransferase from F. x ananassa and Several Alcohol Substrates: A Computational Study. PLoS ONE, 2016, 11, e0153057.	2.5	20

#	Article	IF	CITATIONS
73	Adenosine A <sub>2A</sub> receptor agonists with potent antiplatelet activity. Platelets, 2018, 29, 292-300.	2.3	20
74	BitClust: Fast Geometrical Clustering of Long Molecular Dynamics Simulations. Journal of Chemical Information and Modeling, 2020, 60, 444-448.	5.4	20
75	Protein radial distribution function (P-RDF) and Bayesian-Regularized Genetic Neural Networks for modeling protein conformational stability: Chymotrypsin inhibitor 2 mutants. Journal of Molecular Graphics and Modelling, 2007, 26, 748-759.	2.4	19
76	Docking and quantitative structure–activity relationship studies for sulfonyl hydrazides as inhibitors of cytosolic human branched-chain amino acid aminotransferase. Molecular Diversity, 2009, 13, 493-500.	3.9	19
77	Effects of β-cyclodextrin-dextran polymer on stability properties of trypsin. Biotechnology and Bioengineering, 2003, 83, 743-747.	3.3	18
78	Investigation of the Differences in Activity between Hydroxycycloalkyl N1 Substituted Pyrazole Derivatives As Inhibitors of B-Raf Kinase by Using Docking, Molecular Dynamics, QM/MM, and Fragment-Based <i>De Novo</i> Design: Study of Binding Mode of Diastereomer Compounds. Journal of Chemical Information and Modeling, 2011, 51, 2920-2931.	5.4	18
79	Binding Studies and Quantitative Structure–Activity Relationship of 3â€Aminoâ€1 <i>H</i> â€Indazoles as Inhibitors of GSK3β. Chemical Biology and Drug Design, 2011, 78, 631-641.	3.2	18
80	A coumarinylaldoxime as a specific sensor for Cu2+ and its biological application. Tetrahedron Letters, 2014, 55, 873-876.	1.4	18
81	Mycobacterium tuberculosis serine/threonine protein kinases: structural information for the design of their specific ATP-competitive inhibitors. Journal of Computer-Aided Molecular Design, 2018, 32, 1315-1336.	2.9	18
82	Estimation of 2D autocorrelation descriptors and 2D Monte Carlo descriptors as a tool to build up predictive models for acetylcholinesterase (AChE) inhibitory activity. Chemometrics and Intelligent Laboratory Systems, 2019, 184, 14-21.	3.5	18
83	QSAR models for predicting the activity of non-peptide luteinizing hormone-releasing hormone (LHRH) antagonists derived from erythromycin A using quantum chemical properties. Journal of Molecular Modeling, 2007, 13, 465-476.	1.8	17
84	Ultrasound-assisted phase-transfer catalysis method in an aqueous medium to promote the Knoevenagel reaction: Advantages over the conventional and microwave-assisted solvent-free/catalyst-free method. Ultrasonics Sonochemistry, 2014, 21, 1666-1674.	8.2	17
85	Analyzing torquoselectivity in electrocyclic ring opening reactions of trans-3,4-dimethylcyclobutene and 3-formylcyclobutene through electronic structure principles. Physical Chemistry Chemical Physics, 2015, 17, 23104-23111.	2.8	17
86	K2P channels in plants and animals. Pflugers Archiv European Journal of Physiology, 2015, 467, 1091-1104.	2.8	17
87	Study of the Affinity between the Protein Kinase PKA and Peptide Substrates Derived from Kemptide Using Molecular Dynamics Simulations and MM/GBSA. PLoS ONE, 2014, 9, e109639.	2.5	17
88	A computational ONIOM model for the description of the H-bond interactions between NU2058 analogues and CDK2 active site. Chemical Physics Letters, 2009, 479, 149-155.	2.6	16
89	1â€Benzylâ€1,2,3,4â€Tetrahydroâ€Î²â€Carboline as Channel Blocker of <i>N</i> â€Methylâ€ <scp>d</scp> â€As Receptors. Chemical Biology and Drug Design, 2012, 79, 594-599.	partate 3.2	16
90	Discovery of Novel TASK-3 Channel Blockers Using a Pharmacophore-Based Virtual Screening. International Journal of Molecular Sciences, 2019, 20, 4014.	4.1	16

#	Article	IF	CITATIONS
91	Genetic neural network modeling of the selective inhibition of the intermediate-conductance Ca2+-activated K+ channel by some triarylmethanes using topological charge indexes descriptors. Journal of Computer-Aided Molecular Design, 2005, 19, 771-789.	2.9	15
92	Studying the phosphoryl transfer mechanism of the <i>E. coli</i> phosphofructokinase-2: from X-ray structure to quantum mechanics/molecular mechanics simulations. Chemical Science, 2019, 10, 2882-2892.	7.4	15
93	Docking, Interaction Fingerprint, and Three-Dimensional Quantitative Structure–Activity Relationship (3D-QSAR) of Sigma1 Receptor Ligands, Analogs of the Neuroprotective Agent RC-33. Frontiers in Chemistry, 2019, 7, 496.	3.6	14
94	In silico Comparison of Antimycobacterial Natural Products with Known Antituberculosis Drugs. Journal of Chemical Information and Modeling, 2013, 53, 649-660.	5.4	13
95	Understanding the comparative molecular field analysis (CoMFA) in terms of molecular quantum similarity and DFT-based reactivity descriptors. Journal of Molecular Modeling, 2015, 21, 156.	1.8	13
96	Synthesis of the Indolo[2,3-a]quinolizidine Ring through the Addition of 2-Siloxyfurans to Imines and Intrinsic Reaction Coordinate Calculations. Synthesis, 2012, 44, 144-150.	2.3	12
97	The Dynamic Nonprime Binding of Sampatrilat to the C-Domain of Angiotensin-Converting Enzyme. Journal of Chemical Information and Modeling, 2016, 56, 2486-2494.	5.4	12
98	Synthesis and in silico analysis of the quantitative structure–activity relationship of heteroaryl–acrylonitriles as AChE inhibitors. Journal of the Taiwan Institute of Chemical Engineers, 2016, 59, 45-60.	5.3	12
99	In-Silico Design, Synthesis and Evaluation of a Nanostructured Hydrogel as a Dimethoate Removal Agent. Nanomaterials, 2018, 8, 23.	4.1	12
100	1,3â€Dipolar Cycloaddition of Nitrile Imines with Cyclic αâ€Î²â€Unsaturated Ketones: A Regiochemical Route to Ringâ€Fused Pyrazoles. European Journal of Organic Chemistry, 2011, 2011, 4806-4813.	2.4	11
101	Structural Requirements of N-alpha-Mercaptoacetyl Dipeptide (NAMdP) Inhibitors of Pseudomonas Aeruginosa Virulence Factor LasB: 3D-QSAR, Molecular Docking, and Interaction Fingerprint Studies. International Journal of Molecular Sciences, 2019, 20, 6133.	4.1	11
102	Development of indazolylpyrimidine derivatives as high-affine EphB4 receptor ligands and potential PET radiotracers. Bioorganic and Medicinal Chemistry, 2015, 23, 6025-6035.	3.0	10
103	A study of the cis–trans isomerization preference of N-alkylated peptides containing phosphorus in the side chain and backbone. New Journal of Chemistry, 2019, 43, 12804-12813.	2.8	10
104	New Insights into the Opening of the Occluded Ligand-Binding Pocket of Sigma1 Receptor: Binding of a Novel Bivalent RC-33 Derivative. Journal of Chemical Information and Modeling, 2020, 60, 756-765.	5.4	10
105	Coarse-Grained Parameters for Divalent Cations within the SIRAH Force Field. Journal of Chemical Information and Modeling, 2020, 60, 3935-3943.	5.4	10
106	Study of the interactions between Edaglitazone and Ciglitazone with PPARÎ <sup>3</sup> and their antiplatelet profile. Life Sciences, 2017, 186, 59-65.	4.3	9
107	On the Nature of the Enzyme–Substrate Complex and the Reaction Mechanism in Human Arginase I. A Combined Molecular Dynamics and QM/MM Study. ACS Catalysis, 2020, 10, 8321-8333.	11.2	9
108	Improved Pharmacological Properties for Superoxide Dismutase Modified with Carboxymethycellulose. Journal of Bioactive and Compatible Polymers, 2005, 20, 557-570.	2.1	8

#	Article	IF	CITATIONS
109	Analyses of Synthetic <i>N</i> -Acyl Dopamine Derivatives Revealing Different Structural Requirements for Their Anti-inflammatory and Transient-Receptor-Potential-Channel-of-the-Vanilloid-Receptor-Subfamily-Subtype-1 (TRPV1)-Activating Properties. Journal of Medicinal Chemistry, 2018, 61, 3126-3137.	6.4	8
110	Mechanistic insights into the phosphoryl transfer reaction in cyclin-dependent kinase 2: A QM/MM study. PLoS ONE, 2019, 14, e0215793.	2.5	8
111	Continental and Antarctic Lichens: isolation, identification and molecular modeling of the depside tenuiorin from the Antarctic lichen <i>Umbilicaria antarctica</i> as tau protein inhibitor. Natural Product Research, 2020, 34, 646-650.	1.8	8
112	Analysis of protegrin structure–activity relationships: the structural characteristics important for antimicrobial activity using smoothed amino acid sequence descriptors. Molecular Simulation, 2007, 33, 689-702.	2.0	7
113	Quantitative Structure?Activity Relationship Modeling of Growth Hormone Secretagogues Agonist Activity of some Tetrahydroisoquinoline 1-Carboxamides. Chemical Biology and Drug Design, 2007, 69, 48-55.	3.2	7
114	Inclusion complexes containing poly(É>-caprolactone)diol and cyclodextrins. Experimental and theoretical studies. Polymer, 2009, 50, 2926-2932.	3.8	7
115	Quantitative Structure–Activity Relationship of Organosulphur Compounds as Soybean 15â€Lipoxygenase Inhibitors Using CoMFA and CoMSIA. Chemical Biology and Drug Design, 2010, 76, 511-517.	3.2	7
116	Identification of Mycobacterium tuberculosis CtpF as a target for designing new antituberculous compounds. Bioorganic and Medicinal Chemistry, 2020, 28, 115256.	3.0	7
117	Improved pharmacological properties for superoxide dismutase modified with mannan. Biotechnology and Applied Biochemistry, 2006, 44, 159.	3.1	6
118	Docking and quantitative structure–activity relationship studies for imidazo[1,2-a]pyrazines as inhibitors of checkpoint kinase-1. Medicinal Chemistry Research, 2012, 21, 1912-1920.	2.4	6
119	New insights into steric and electronic effects in a series of phosphine ligands from the perspective of local quantum similarity using the Fukui function. Journal of Molecular Modeling, 2015, 21, 45.	1.8	6
120	Study of the affinity between the protein kinase PKA and homoarginineâ€containing peptides derived from kemptide: Free energy perturbation (FEP) calculations. Journal of Computational Chemistry, 2018, 39, 986-992.	3.3	6
121	Insights into the Structural Requirements of 2(S)-Amino-6-Boronohexanoic Acid Derivatives as Arginase I Inhibitors: 3D-QSAR, Docking, and Interaction Fingerprint Studies. International Journal of Molecular Sciences, 2018, 19, 2956.	4.1	6
122	Chalcone derivatives as non-canonical ligands of TRPV1. International Journal of Biochemistry and Cell Biology, 2019, 112, 18-23.	2.8	6
123	Dammarane triterpenes targeting α-synuclein: biological activity and evaluation of binding sites by molecular docking. Journal of Enzyme Inhibition and Medicinal Chemistry, 2021, 36, 154-162.	5.2	6
124	Computational Modeling to Explain Why 5,5-Diarylpentadienamides are TRPV1 Antagonists. Molecules, 2021, 26, 1765.	3.8	6
125	Bitopic Sigma 1 Receptor Modulators to Shed Light on Molecular Mechanisms Underpinning Ligand Binding and Receptor Oligomerization. Journal of Medicinal Chemistry, 2021, 64, 14997-15016.	6.4	6
126	A CoMSIA study on the adenosine kinase inhibition of pyrrolo[2,3-d]pyrimidine nucleoside analogues. Bioorganic and Medicinal Chemistry, 2008, 16, 5103-5108.	3.0	5

#	Article	IF	CITATIONS
127	Proteochemometric Modeling of the Inhibition Complexes of Matrix Metalloproteinases with <i>N</i> â€Hydroxyâ€2â€{(Phenylsulfonyl)Amino]Acetamide Derivatives Using Topological Autocorrelation Interaction Matrix and Model Ensemble Averaging. Chemical Biology and Drug Design, 2008, 72, 65-78.	3.2	5
128	Synthesis of coumarin derivatives as fluorescent probes for membrane and cell dynamics studies. European Journal of Medicinal Chemistry, 2014, 76, 79-86.	5.5	5
129	Optimal graphâ€based and Simplified Molecular Input Line Entry Systemâ€based descriptors for quantitative structure–activity relationship analysis of arylalkylaminoalcohols, arylalkenylamines, and arylalkylamines as Ïf < sub> 1 < /sub> receptor ligands. Journal of Chemometrics, 2015, 29, 13-20.	1.3	5
130	Radiofluorinated <i>N</i> -Octanoyl Dopamine ([ <sup>18</sup> F]F-NOD) as a Tool To Study Tissue Distribution and Elimination of NOD in Vitro and in Vivo. Journal of Medicinal Chemistry, 2016, 59, 9855-9865.	6.4	5
131	Docking and quantitative structure–activity relationship of bi-cyclic heteroaromatic pyridazinone and pyrazolone derivatives as phosphodiesterase 3A (PDE3A) inhibitors. PLoS ONE, 2017, 12, e0189213.	2.5	5
132	PSIQUE: Protein Secondary Structure Identification on the Basis of Quaternions and Electronic Structure Calculations. Journal of Chemical Information and Modeling, 2021, 61, 1789-1800.	5.4	5
133	Classification of conformational stability of protein mutants from 2D graph representation of protein sequences using support vector machines. Molecular Simulation, 2007, 33, 889-896.	2.0	4
134	Comparative modeling of the conformational stability of chymotrypsin inhibitor 2 protein mutants using amino acid sequence autocorrelation (AASA) and amino acid 3D autocorrelation (AA3DA) vectors and ensembles of Bayesian-regularized genetic neural networks. Molecular Simulation, 2007, 33, 1045-1056.	2.0	4
135	Modeling of the Inhibition of the Intermediate onductance Ca <sup>2+</sup> â€Activated K <sup>+</sup> Channel (IKCa1) by Some Triarylmethanes Using Quantum Chemical Properties Derived From <i>Ab Initio</i> Calculations. QSAR and Combinatorial Science, 2008, 27, 866-875.	1.4	4
136	Models of the pharmacophoric pattern and affinity trend of methyl 2-(aminomethyl)-1-phenylcyclopropane-1-carboxylate derivatives as σ <sub>1</sub> ligands. Molecular Simulation, 2012, 38, 227-235.	2.0	4
137	HQSAR and molecular docking studies of furanyl derivatives as adenosine A2A receptor antagonists. Medicinal Chemistry Research, 2016, 25, 1316-1328.	2.4	4
138	BitQT: a graph-based approach to the quality threshold clustering of molecular dynamics. Bioinformatics, 2021, 38, 73-79.	4.1	4
139	RCDPeaks: memory-efficient density peaks clustering of long molecular dynamics. Bioinformatics, 2022, 38, 1863-1869.	4.1	4
140	Proteometric modelling of protein conformational stability using amino acid sequence autocorrelation vectors and genetic algorithm-optimised support vector machines. Molecular Simulation, 2008, 34, 857-872.	2.0	3
141	Transforming Non-Selective Angiotensin-Converting Enzyme Inhibitors in C- and N-domain Selective Inhibitors by Using Computational Tools. Mini-Reviews in Medicinal Chemistry, 2020, 20, 1436-1446.	2.4	3
142	SAR and QSAR Modeling of Juvenile Hormone Mimics. , 2013, , 159-188.		2
143	Molecular Modeling of Tau Proline-Directed Protein Kinase (PDPK) Inhibitors. Neuromethods, 2018, , 305-345.	0.3	2
144	Energetic differences between non-domain-swapped and domain-swapped chain connectivities in the K2P potassium channel TRAAK. RSC Advances, 2018, 8, 26610-26618.	3.6	2

#	Article	IF	CITATIONS
145	3D-QSAR Modeling of Non-peptide Antagonists for the Human Luteinizing Hormone-releasing Hormone Receptor. Medicinal Chemistry, 2013, 9, 560-570.	1.5	2
146	Graphical Representations of Protein Sequences for Alignment-Free Comparative and Predictive Studies. Recognition of Protease Inhibition Pattern from H-Depleted Molecular Graph Representation of Protease Sequences. Current Bioinformatics, 2010, 5, 241-252.	1.5	2
147	Easy Identification of Residues Involved on Structural Differences Between Nonphosphorylated and Phosphorylated CDK2Cyclin A Complexes Using Twoâ€Dimensional Networks. Molecular Informatics, 2014, 33, 151-162.	2.5	1
148	Genetic Algorithm Optimization of Bayesian-Regularized Artificial Neural Networks in Drug Design. , 2016, , 83-102.		1
149	Predicting the stability of human lysozyme mutants using the tree-based classifier TTOSOM. Chemometrics and Intelligent Laboratory Systems, 2017, 162, 65-72.	3.5	1
150	Synthesis of diN-Substituted Glycyl-Phenylalanine Derivatives by Using Ugi Four Component Reaction and Their Potential as Acetylcholinesterase Inhibitors. Molecules, 2019, 24, 189.	3.8	1
151	Multiâ€scale simulation reveals that an amino acid substitution increases photosensitizing reaction inputs in Rhodopsins. Journal of Computational Chemistry, 2020, 41, 2278-2295.	3.3	1

152 Editorial [Hot Topic: Protein Kinase Inhibitors: Current Strategies and Future Prospects (Executive) Tj ETQq0 0 0 rgBT/Overlock 10 Tf 50

153	Kristallographie - New Crystal Structures, 2016, 231, 171-173.	0.3	0
154	<strong>Free energy theoretical calculations of PKA–Kemptide complex formation, and effect of mutation of Kemptide arginines to homoarginines.</strong> ., 0, , .		0